PACS numbers: 42.55.Tv, 42.60.Da
DOI: 10.1070/QE2009v039n12ABEH014164

Two-dimensional distributed feedback lasers with excitation of TE waves in the active medium

V.R. Baryshev, N.S. Ginzburg, A.M. Malkin, A.S. Sergeev

***Abstract*. Two-dimensional Bragg resonators with the coupling of TE- and TM-polarised waves are proposed. The selective properties of such resonators are analysed. Within the semiclassical approach, the nonlinear dynamics of laser radiation with a two-dimensional (in the xy plane) distributed feedback is studied, at which TE-polarised waves, propagating in the $\pm z$ directions, are amplified in the active medium (in particular, based on quantum wells). The latter, on a two-dimensional Bragg structure, are scattered into TM-polarised waves propagating in the $\pm x$ directions. These partial wave flows do not interact with the active medium but provide the spatial radiation synchronisation. The conditions of the solution self-similarity are obtained with increasing the dimensions of the active medium and the corresponding increase in the integral output power. It is shown that when an additional end mirror is mounted, almost unidirectional radiation coupling can be realised.**

Keywords: *distributed feedback lasers, two-dimensional Bragg resonator, mode selection.*

1. Introduction

Conventional distributed feedback (DFB) lasers use the coupling of two counterpropagating waveguide modes in a structure with a periodic modulation of dielectric properties [1 – 7]. Such a structure forms a one-dimensional Bragg resonator, which allows one to selects modes with respect to the longitudinal index. Transverse synchronisation of radiation can be provided by diffraction if the transverse size l_x of the system is limited by the Fresnel condition: $l_x^2/(l_z\lambda) \leqslant 1$, where l_z is the system length; λ is the radiation wavelength. The authors of papers [8–10] proposed an efficient method for spatial synchronisation of radiation in the case of a large Fresnel parameter $[l_x^2/(l_z\lambda) \gg 1]$, based on the use of a two-dimensional DFB.

In the optical range, a two-dimensional DFB can be produced using dielectric structures with a doubly periodic modulation of the waveguide thickness (Fig. 1a, b):

V.R. Baryshev, N.S. Ginzburg, A.M. Malkin, A.S. Sergeev Institute of Applied Physics, Russian Academy of Sciences, ul. Ul'yanova 46, 603950 Nizhnii Novgorod, Russia; e-mail: baryshev@appl.sci-nnov.rus

Received 8 June 2009; revision received 7 September 2009
Kvantovaya Elektronika **39** (12) 1159 – 1164 (2009)
Translated by I.A. Ulitkin

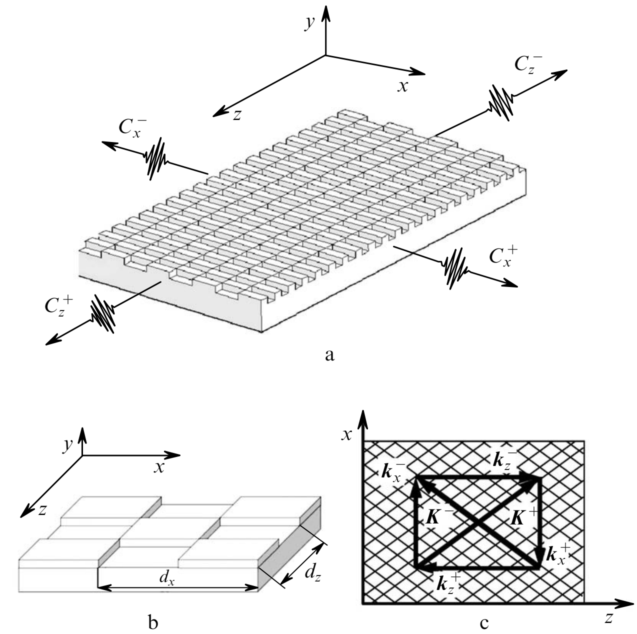

Figure 1. General scheme of a two-dimensional DFB laser (a), chess-like approximation of the dielectric waveguide surface on an enlarged scale (b) and diagram illustrating the coupling of the partial waves ($\boldsymbol{k}_x^{\pm} = \mp h_x \boldsymbol{x}_0$ and $\boldsymbol{k}_z^{\pm} = \mp h_z \boldsymbol{z}_0$ are the wave vectors of the partial waves, $\boldsymbol{K}^{\pm} = \bar{h}_x \boldsymbol{x}_0 \pm \bar{h}_z \boldsymbol{z}_0$ are the translation vectors of the grating, $\boldsymbol{x}_0$, $\boldsymbol{z}_0$ are unit vectors).

$$b(x,z) = b_0 + b_1\left[\cos\left(\bar{h}_x x + \bar{h}_z z\right) + \cos\left(\bar{h}_x x - \bar{h}_z z\right)\right], \quad (1)$$

where b_1 is the modulation amplitude; $\bar{h}_{x,z} = 2\pi/d_{x,z}$; $d_{x,z}$ are the modulation periods along the x and z axes. Such structures provide coupling and mutual scattering of four partial wave flows specified by the vector-potential

$$\boldsymbol{A} = \mathrm{Re}\Big\{\big[\boldsymbol{a}_z(y)\big(C_z^+ \mathrm{e}^{-\mathrm{i}h_z z} + C_z^- \mathrm{e}^{\mathrm{i}h_z z}\big) + \boldsymbol{a}_x(y)\big(C_x^+ \mathrm{e}^{-\mathrm{i}h_x x} + C_x^- \mathrm{e}^{\mathrm{i}h_x x}\big)\big]\mathrm{e}^{\mathrm{i}\omega t}\Big\}, \quad (2)$$

where the functions $\boldsymbol{a}_{x,z}(y)$ describe the known mode structure of a regular planar waveguide with a dielectric constant [3], the modes propagating in the directions $\pm x$ and $\pm z$ with the moduli h_x and h_z of the wave vectors; $C_{x,z}^{\pm}(x,z)$ are the slowly-varying complex amplitudes of the partial waves. We assume that the Bragg conditions (Fig. 1c) $h_{x,z} \approx \bar{h}_{x,z}$ are fulfilled under which the waves with the amplitudes $C_z^{\pm}$ propagating in the directions $\pm z$ are coupled with the waves with the amplitudes $C_x^{\pm}$

propagating in the directions $\pm x$. Note that the direct coupling between the waves C_z^+ and C_z^-, as well as between C_x^+ and C_x^- are absent.

In practical realisation, similarly to the case of two-dimensional Bragg resonators based on the coupling of TM waves [8–10], sinusoidal modulation can be replaced by the chess-like modulation (Fig. 1b):

$$b_{x,z} = b_0 + b_1 f(x) f(z),$$
$$f(\zeta) = \begin{cases} 1, & q\pi/\bar{h}_\zeta < (2q+1)\pi/\bar{h}_\zeta, \\ -1, & (2q+1)\pi/\bar{h}_\zeta < \zeta, 2q\pi/\bar{h}_\zeta, \end{cases} \quad (3)$$

where $q = 1, 2, \ldots$.

Note that in our previous papers [8–10], we considered the case when all four partial wave flows represented TM-polarised waves. The eigenmodes of this resonator are described in detail in paper [10], which shows a high selectivity of such resonators along two coordinates at large Fresnel parameters. The nonlinear dynamics of a two-dimensional DFB laser was studied in [8, 9] by assuming that all the waves refer to one TM type and the laser active medium ensures their isotropic amplification. As is known, the interaction with the TM-polarised waves takes place in semiconductor active media. At the same time, in active media based on quantum wells, TE-polarised waves are mainly amplified [11]. However, due to the orthogonality of electric fields of partial waves, coupling on a two-dimensional Bragg structure (1) of TE-polarised waves is absent (see below).

In this paper, to overcome the mentioned polarisation restrictions we study the two-dimensional DFB laser model with the coupling of TE- and TM-polarised waves. We assume that the active medium amplifies the TE-polarised waves propagating in the directions $\pm z$, these waves being scattered on the Bragg structure into the TM-polarised waves propagating in the directions $\pm z$. These partial wave flows do not interact with the active medium but provide the spatial synchronisation of radiation.

2. Modes of a two-dimensional Bragg resonator with the coupling of TE- and TM-polarised waves

The eigenmodes of a planar dielectric waveguide separate TE- and TM-polarised waves (see, for example, [3]). Papers [8, 9] studied the coupling on a two-dimensional Bragg structure (1) of TM-polarised waves for which the partial waves $C_x^\pm$ and $C_z^\pm$ have a common electric field component (E_y) and correspondingly a different-from-zero coupling coefficient (this coefficient is proportional to the scalar product of the electric fields of the partial waves [3]). In the case of the TE-polarised waves, the electric field is directed perpendicular to the wave vector; hence, the electric fields of the waves $C_x^\pm$ and $C_z^\pm$ are orthogonal and the coupling between the waves is absent. However, as was noted above, in the active medium formed by the quantum wells, it is the TE-polarised waves that are amplified. In this case, of interest is the situation where the coupling of TE and TM waves, propagating in mutually perpendicular directions, is realised on a two-dimensional Bragg grating. The electric field of the TM wave has a longitudinal component, which provides their coupling with TE waves. The waveguide thickness should be selected so that in the studied frequency range specified by the working transition frequency, only the lowest TE and TM modes would propagate in the waveguide.

The coupled-wave equations describing mutual scattering of partial TE and TM waves on a two-dimensional Bragg grating can be reduced, in the geometric optics approximation (the case of large Fresnel parameters), to the form used in [8–10] to describe the scattering of TM waves:

$$\frac{\partial \tilde{C}_z^\pm}{\partial \tilde{z}} \pm i\delta \tilde{C}_z^\pm \pm i\alpha\bar{k}\left(\tilde{C}_x^+ + \tilde{C}_x^-\right) = 0,$$
$$\frac{\partial \tilde{C}_x^\pm}{\partial \tilde{x}} \pm i\delta \tilde{C}_x^\pm \pm i\alpha\bar{k}\left(\tilde{C}_z^+ + \tilde{C}_z^-\right) = 0. \quad (4)$$

Here, $\delta = (\omega - \bar{\omega})/v_g$ is the Bragg resonance detuning; $\tilde{x} = xr^{-1}$; $\tilde{z} = zr$; $r = \sqrt{v_{gx}/v_{gz}}$; $v_g = \sqrt{v_{gx}v_{gz}}$; v_{gx} and v_{gz} are the group velocities of the lowest TE (the subscript z) and TM (the subscript x) modes of the dielectric waveguide; $\tilde{C}_x^\pm = C_x^\pm r^{-1/2}$; $\tilde{C}_z^\pm = C_z^\pm r^{1/2}$; $\bar{k} = \bar{\omega}/c$; $\bar{\omega}$ is the Bragg frequency. The coupling parameter α, following [3], can be represented in the form

$$\alpha = \frac{vb_1}{\sqrt{b^{\rm TE}b^{\rm TM}}} \frac{\sqrt{\varepsilon - 1}(\varepsilon^2 + 1)}{8\sqrt{\varepsilon}} \left(\frac{g_z p_z}{\sqrt{h_z^3}}\right) \times \left(\frac{p_x}{\sqrt{h_x(g_x^2 + \varepsilon^2 p_z^2)}}\right), \quad (5)$$

where

$$b^{\rm TE} = b_0 + \frac{2}{\sqrt{h_z^2 - \bar{k}^2}},$$
$$b^{\rm TM} = b_0 + \frac{2}{\sqrt{h_x^2 - \bar{k}^2}\left[h_x^2/(\varepsilon\bar{k}^2) + h_x^2/\bar{k}^2 - 1\right]}$$

are the effective waveguide thicknesses for TE and TM modes; $p_{x,z}^2 = h_{x,z}^2 - \bar{k}^2$, $g_{x,z}^2 = \varepsilon\bar{k}^2 - h_{x,z}^2$ are the transverse (along the y axis) wave numbers outside and inside the dielectric layer, respectively, for TE and TM modes. In the case of the sinusoidal modulation, $v = 1$, and in the case of chess-like modulation, $v = 16/\pi^2$. The functions $\boldsymbol{a}_z(y)$ and $\boldsymbol{a}_x(y)$ describing the transverse structures of partial TE and TM waves, respectively, are normalised as follows:

$$|\boldsymbol{a}_z(y=0)| = 1, \quad \int \varepsilon|\boldsymbol{a}_z(y)|{\rm d}y = \int \varepsilon|\boldsymbol{a}_x(y)|{\rm d}y.$$

The spectrum of the resonator eigenmodes can be found from the solution of the system of equations (4) with boundary conditions

$$\tilde{C}_z^+(\tilde{x}, 0) = 0,\ \tilde{C}_z^-(\tilde{x}, \tilde{z}) = 0,\ \tilde{C}_x^+(0, \tilde{z}) = 0,\ \tilde{C}_x^-(\tilde{l}_x, \tilde{z}) = 0, \quad (6)$$

which correspond to the absence of incident external electromagnetic fluxes. Here, $\tilde{l}_{x,z} = l_{x,z}r^{\pm 1}$ is the length and width of the region occupied by the two-dimensional modulation with the sinusoidal (1) and chess-like (3) surface profile.

The eigenmode frequencies $\omega_{nm} \approx \bar{\omega} + v_g{\rm Re}\delta_{mn}$ and their Q factors $Q_{mn} \approx \bar{\omega}/(2v_g{\rm Im}\delta_{mn}))$ in the case of strong coupling ($\alpha\bar{k}\tilde{l}_{x,z} \gg 1$) can be represented in the form [10]

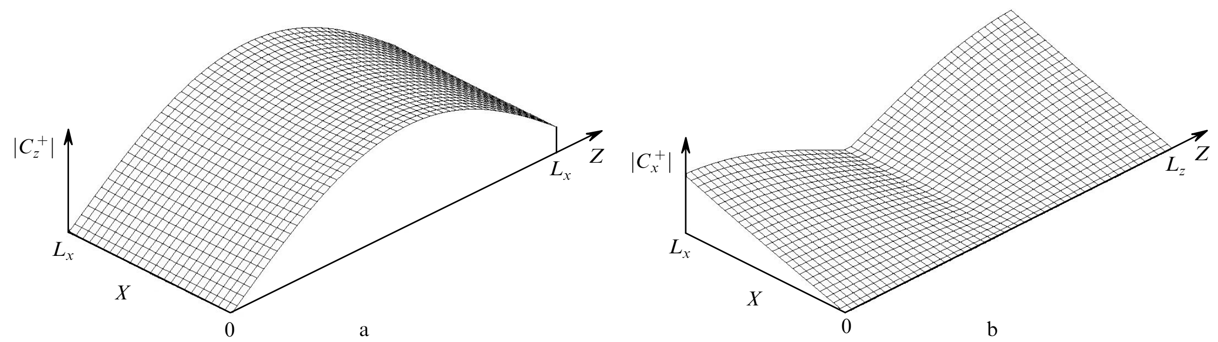

Figure 2. Field structures of the partial waves C_z^+ (a) and C_x^+ (b) of the fundamental mode ($n = 0$, $m = 1$) at $L_z = 5$, $L_x = 2.5$.

$$\delta_{mn} = \pm\left[2\alpha\bar{k} + \frac{\pi^2}{4\alpha\bar{k}}\left(\frac{n^2}{\bar{l}_z^2} + \frac{m^2}{\bar{l}_x^2}\right)\right] + \mathrm{i}\,\frac{\pi^2}{2\alpha^2\bar{k}^2}\left(\frac{n^2}{\bar{l}_z^3} + \frac{m^2}{\bar{l}_x^3}\right), \tag{7a}$$

$$\delta_{mn} = \pm\frac{\pi^2 mn}{2\alpha\bar{k}\tilde{l}_z\tilde{l}_x} + \mathrm{i}\,\frac{\pi^2}{2\alpha^2\bar{k}^2\tilde{l}_z\tilde{l}_x}\left(\frac{n^2}{\tilde{l}_z} + \frac{m^2}{\tilde{l}_x}\right). \tag{7b}$$

According to (7), the studied modification of the two-dimensional Bragg resonator has a high selectivity over the longitudinal (n) and transverse (m) subscripts, the selectivity being achieved due to the simultaneous coupling of radiation both in the longitudinal ($\pm z$) and transverse ($\pm x$) directions. The eigenmodes can be divided into two groups whose frequencies lie near the boundaries of the Bragg band: $\delta \approx \pm 2\alpha\bar{k}$ (7a) and in the vicinity of the exact Bragg resonance: $\delta = 0$ (7b). A distinct feature of two-dimensional Bragg structures is the existence of high-Q modes from the second group inside the Bragg band. The modes at the exact Bragg frequency with the subscripts $m = 0$, $n = 1$ and $m = 1$, $n = 0$ have the highest-Q factor. Within the framework of the geometric optics approximation, these modes are degenerate with respect to the frequency, and, in addition, at $\tilde{l}_x = \tilde{l}_z$, they have the same Q factor. To remove the degeneracy with respect to the Q factor, we will consider below the systems with $\tilde{l}_z = 2\tilde{l}_x$. The spatial amplitude distributions of the partial waves of the fundamental mode ($m = 0$, $n = 1$) are shown in Fig. 2 for this case.

3. Simulation of nonlinear dynamics of two-dimensional DFB lasers

Let a thin (in the scale of the waveguide mode inhomogeneities) layer of the active medium be located at the plate centre at $y = 0$ and interact only with TE-polarised waves. We assume that the Bragg frequency $\bar{\omega}$ coincides with the transition frequency ω_0 between the working levels. We will describe the interaction of the active medium with the electromagnetic field within the framework of the semiclassical approach [12]. Thus, in the expression for the electromagnetic field (2) in which the amplitudes of the partial wave flows $C_{x,z}^{\pm}$ are also the time functions, the polarisation P and population inversion ρ of the medium will be represented in the form [12]

$$P = \mathrm{Re}\left[\mathrm{i}\left(P_z^+ \mathrm{e}^{\mathrm{i}\bar{h}z} + P_z^- \mathrm{e}^{-\mathrm{i}\bar{h}z}\right)\mathrm{e}^{\mathrm{i}\omega_0 t}\right],$$
$$\rho = \rho_0 + \mathrm{Re}\left(\rho_{2z}\mathrm{e}^{2\mathrm{i}\bar{h}z}\right), \tag{8}$$

where $P_z^{\pm}(x, z, t)$, $\rho_0(x, z, t)$, $\rho_{2z}(x, z, t)$ are the slowly varying amplitudes of the corresponding spatial harmonics.

The process of partial wave amplification (2) in the active medium and their mutual re-scattering on the Bragg grating (1) and nonlinear grating produced by the population inversion modulation of the medium can be described by a system of averaged equations:

$$\left(\pm\frac{\partial}{\partial Z} + \frac{\partial}{\partial \tau}\right)\hat{C}_z^{\pm} + \mathrm{i}\left(\hat{C}_x^+ + \hat{C}_x^-\right) = \hat{P}_z^{\pm},$$
$$\left(\pm\frac{\partial}{\partial X} + \frac{\partial}{\partial \tau}\right)\hat{C}_x^{\pm} + \mathrm{i}\left(\hat{C}_z^+ + \hat{C}_z^-\right) = 0,$$
$$\frac{\partial\hat{\rho}_0}{\partial\tau} + \frac{\hat{\rho}_0 - 1}{\hat{T}_1} = -\mathrm{Re}\left(\hat{C}_z^+\hat{P}_z^{+*} + \hat{C}_z^-\hat{P}_z^{-*}\right),$$
$$\frac{\partial\hat{\rho}_{2z}}{\partial\tau} + \frac{\hat{\rho}_{2z}}{\hat{T}_1} = -\left(\hat{C}_z^+\hat{P}_z^{-*} + \hat{C}_z^-\hat{P}_z^{+*}\right). \tag{9}$$

Here, $X = \alpha\omega_0 x r^{-1}/c$, $Z = \alpha\omega_0 z r/c$, $\tau = \alpha\omega_0 t v_{\mathrm{g}}/c$ are the normalised spatial coordinates and time;

$$\hat{\rho}_{0,2z} = \frac{\rho_{0,2z}}{\rho_{\mathrm{e}}};\quad \hat{P}_z^{\pm} = P_z^{\pm}\left(\frac{\pi b_0 c}{\alpha\rho_{\mathrm{e}} h\omega_0^3 v_{\mathrm{g}} b^{\mathrm{TE}} r}\right)^{1/2};$$

$$C_x^{\pm} = C_x^{\pm}\left(\frac{b^{\mathrm{TE}}\omega_0}{\pi\rho_{\mathrm{e}} h v_{\mathrm{g}} b_0 r c}\right)^{1/2};\quad C_z^{\pm} = C_z^{\pm}\left(\frac{b^{\mathrm{TE}}\omega_0 r}{\pi\rho_{\mathrm{e}} h v_{\mathrm{g}} b_0 r c}\right)^{1/2};$$

$$\hat{T}_{1,2} = \frac{\alpha\omega_0 T_{1,2} v_{\mathrm{g}}}{c};$$

ρ_{e} is the equilibrium concentration of the active elements in the absence of radiation; $T_{1,2}$ are the longitudinal and transverse relaxation times.

Assuming the transverse relaxation time T_2 to be small compared to other temporal scales, we will use the balance approximation by representing the medium polarisation components in the form

$$\hat{P}_z^+ = \beta\hat{T}_2\left(2\hat{C}_z^+\hat{\rho}_0 + \hat{C}_z^-\hat{\rho}_{2z}\right),$$
$$\hat{P}_z^- = \beta\hat{T}_2\left(2\hat{C}_z^-\hat{\rho}_0 + \hat{C}_z^+\hat{\rho}_{2z}^*\right), \tag{10}$$

where

$$\beta = \frac{\pi\rho_{\mathrm{e}}|\mu|^2 c b_0}{2\alpha^2 h\omega_0^3 v_{\mathrm{g}} b^{\mathrm{TE}} r}$$

is the normalised density of the active elements; μ is the dipole moment.

The total output power is

$$S = \frac{\rho_e hc^2 b_0}{4\alpha}\,\hat{S}, \tag{11}$$

where

$$\hat{S} = r^{-1}\int_0^{L_x}\left(\left|\hat{C}_z^{+}(X, L_z)\right|^2 + \left|\hat{C}_z^{-}(X,0)\right|^2\right)\mathrm{d}X + r\int_0^{L_z}\left(\left|\hat{C}_x^{+}(L_x, Z)\right|^2 + \left|\hat{C}_x^{-}(0,Z)\right|^2\right)\mathrm{d}Z; \tag{12}$$

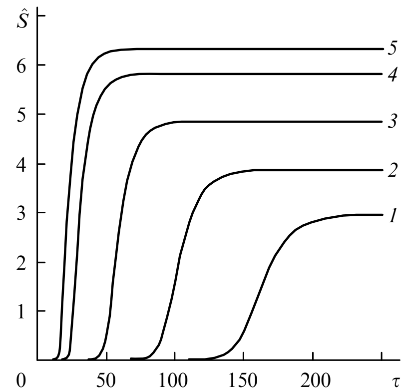

Figure 3. Dependences of the normalised output power $\hat{S}$ on the normalised time τ at $L_z = 5$, $L_x = 2.5$, $\hat{T}_1 = 1$ and excesses over the self-excitation threshold $\beta\hat{T}_2 = 0.075$ (*1*), 0.1 (*2*), 0.15 (*3*), 0.25 (*4*) and 0.35 (*5*).

$L_{x,z} = \alpha\omega_0\tilde{l}_{x,z}/c$ are the normalised width and length of the active medium.

In the strong wave coupling approximation ($L_{x,z} \gg 1$), the conditions for the self-excitation of different modes can be written in the form

$$\mathrm{Im}\,\frac{\delta_{nm}}{\alpha\bar{k}} = 2\beta\hat{T}_2, \tag{13}$$

where the mode decrements are determined by relations (7). The minimal self-excitation threshold F is realised for the fundamental mode and can be represented in the form

$$F = 4\beta\hat{T}_2 L_z^2 L_z/\pi^2 = 1. \tag{14}$$

We studied the nonlinear interaction stage by using the numerical simulation of the system of equation (9), (10) with boundary conditions (6). As initial conditions, we specified the noise distribution of the electromagnetic field with a small amplitude c_0:

$$\hat{C}_{x,z}^{\pm}(X, Z, \tau = 0) = c_0 \exp[-\varphi_{x,z}^{\pm}(X, Z)]. \tag{15}$$

Figure 3 presents the time dependences of the normalised output power $\hat{S}$ at different excesses of the self-excitation threshold. Figure 4 shows the spatiotemporal dependences of the amplitudes and partial wave phases on one of the active region boundaries, which demonstrate the process of radiation synchronisation and establishment of the stationary lasing regime. Amplitude distributions of the partial waves and the mean population inversion in the stationary lasing regime are demonstrated in Fig. 5. Note that the dependences presented in Figs 4 and 5 are obtained

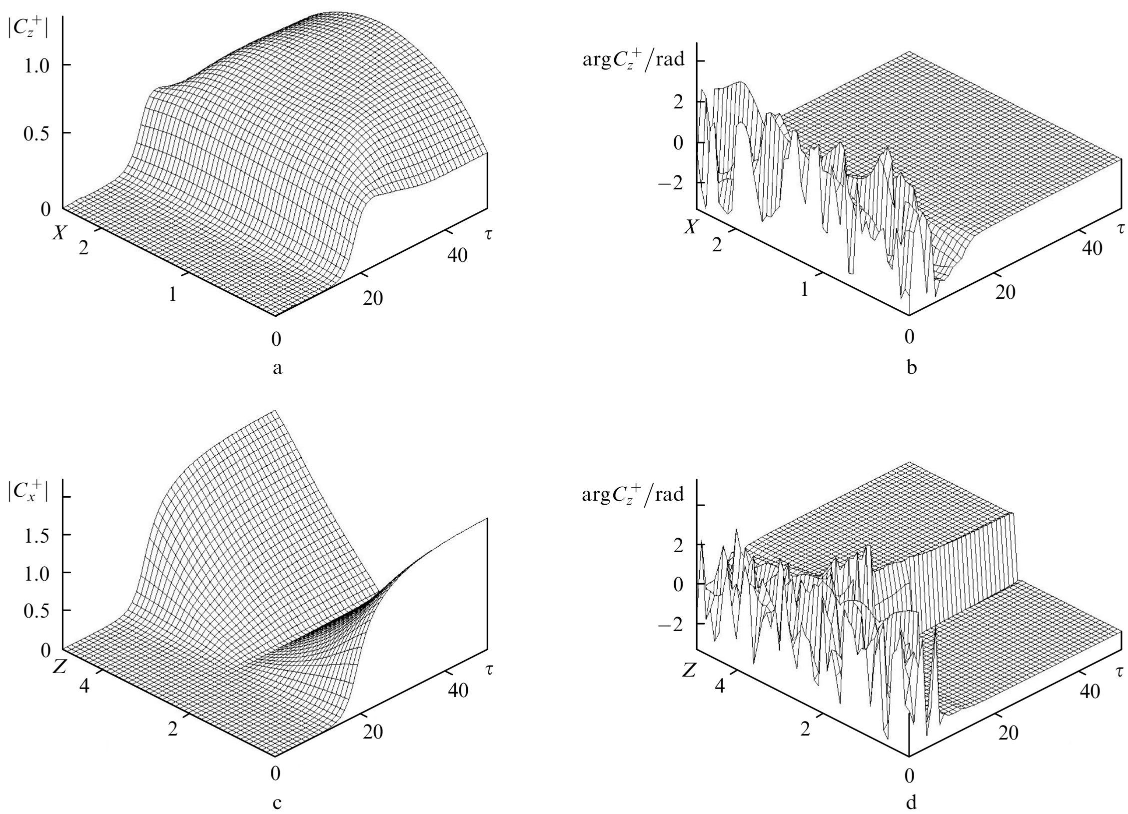

Figure 4. Spatiotemporal dependences of the amplitudes and phases of the partial waves C_z^+ (a, b) and C_x^+ (c, d) on the active region boundaries during the establishment of the stationary lasing regime at $Z = L_z z$ (a, b), $X = L_x$ (c, d), $L_z = 5$, $L_x = 2.5$, $\beta\hat{T}_2 = 0.35$, $\hat{T}_1 = 1$.

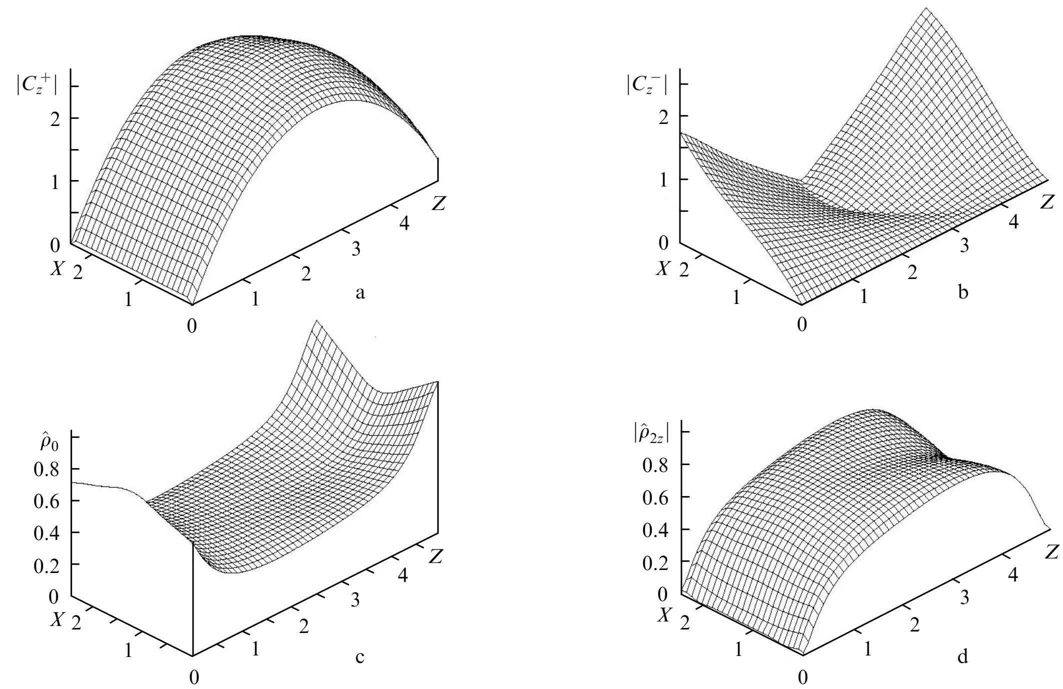

Figure 5. Spatial dependences of the amplitudes of the partial waves C_z^+ (a) and C_x^+ (b), the mean population inversion $\hat{\rho}_0$ (c), and the induced population-inversion grating $|\hat{\rho}_{2z}|$ (d) in the stationary lasing regime at $L_z = 5$, $L_x = 2.5$, $\beta\hat{T}_2 = 0.35$, $\hat{T}_1 = 1$.

at a significant excess of the lasing threshold: $F \approx 9$. Under these conditions, several modes of a two-dimensional Bragg resonator are excited at the initial stage but, due to the nonlinear competition, the stationary lasing regime with the amplitude distributions of partial waves, analogous to the field distribution of the fundamental ($n = 1$, $m = 0$) mode, is established (see Fig. 2).

Note that the stationary solutions of equations (9) are self-similar. If we decrease the normalised relaxation time $\hat{T}_1$ of the population inversion without changing the normalised dimensions of the system ($L_{x,z} = \text{const}$), the amplitude distributions of the partial waves in the stationary lasing regime do not change. At the same time, the wave amplitudes and the normalised output power will increase proportionally: $|\hat{C}_{x,z}^{\pm}|^{1/2}\hat{T}_1 = \text{const}$, $\hat{S}\hat{T}_1 = \text{const}$ (Fig. 6). In physical variables, it means that if the size $l_{x,z}$ of the active region is increased and the equilibrium population inversion ρ_{e} (for example, by decreasing the pump power density) and the coupling coefficient α are proportionally decreased so that $l_{x,z}\rho_{\text{e}} = \text{const}$ and $l_{x,z}\alpha = \text{const}$, the amplitude distribution of the partial waves in the stationary regime will not change and the total integral output power will increase proportionally: $S/l_{x,z} = \text{const}$.

Simulation of the lasing establishment process with the help of equations (9) shows that the dynamics of the transient process changes with varying $\hat{T}_1$ because it determines the ratio between the relaxation time $\hat{T}_1$ and the lifetime of photons in the resonator, $T_{\text{p}} = 1/\text{Im}\delta_{10}$. At $\hat{T}_1 \geqslant T_{\text{p}}$, the transient process includes generation of a pulse with the peak power exceeding significantly the output power in the stationary lasing regime (Fig. 6). When $\hat{T}_1$ is decreased, the dynamics of the transient process becomes simpler. In this case, in the entire range of normalised system dimensions admissible from the point of view of computational resources ($L_{x,z} \leqslant 10$), the establishment of the stationary lasing regime was observed.

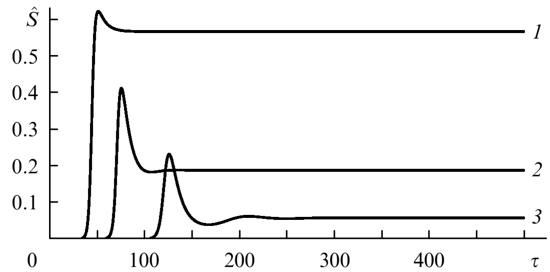

Figure 6. Time dependences of the normalised output power at $L_z = 5$, $L_x = 2.5$, $\beta\hat{T}_2 = 0.1$ and the relaxation constant $\hat{T}_1 = 10$ (*1*), 33 (*2*), and 100 (*3*).

Thus, the simulation results demonstrate the possibility of using two-dimensional distributed Bragg structures for the spatial synchronization of radiation from two-dimensional active media in which the medium amplifies two partial TE-polarised waves propagating in the directions $\pm z$. These waves are scattered on the Bragg structure into TM-polarised waves propagating in the directions $\pm x$, thereby, synchronising radiation of different parts of the active medium.

The disadvantage of the proposed scheme is the radiation coupling from all the four end faces of the active medium. Nevertheless, there exists the possibility to realise an almost unidirectional radiation coupling if we mount an additional end mirror, which will ensure, in the cross section $x = 0$, re-reflection of the wave C_x^- to the wave C_x^+ (Fig. 7). In this case, the boundary condition in this cross section is transformed to the form

$$C_x^+(0, Z) = -RC_x^-(0, Z), \tag{16}$$

where R is the reflection coefficient from the additional end mirror. Figure 8 shows the amplitude distributions of the partial waves obtained during the numerical simulation at

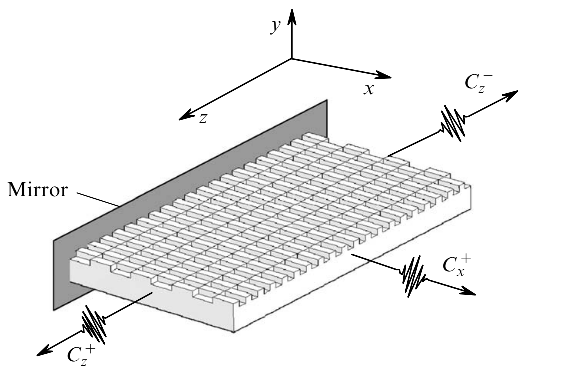

Figure 7. Scheme of a two-dimensional DFB laser with an additional end mirror.

TE waves. The lasing threshold in a two-dimensional DFB laser has been found analytically. We have simulated numerically, within the framework of a semiclassical approximation, the parameters of the stationary lasing regime including the self-similarity conditions. We have demonstrated the possibility providing an almost unidirectional radiation coupling with the help of an additional end mirror.

Acknowledgements. The authors thank V.Ya. Aleshkin, A.A. Andronov, Vl.V. Kocharovskii and E.R. Kocharovskaya for useful discussions. This work was supported by the Russian Foundation for Basic Research (Grant No. 08-08-00966) and the Dynasty Foundation.

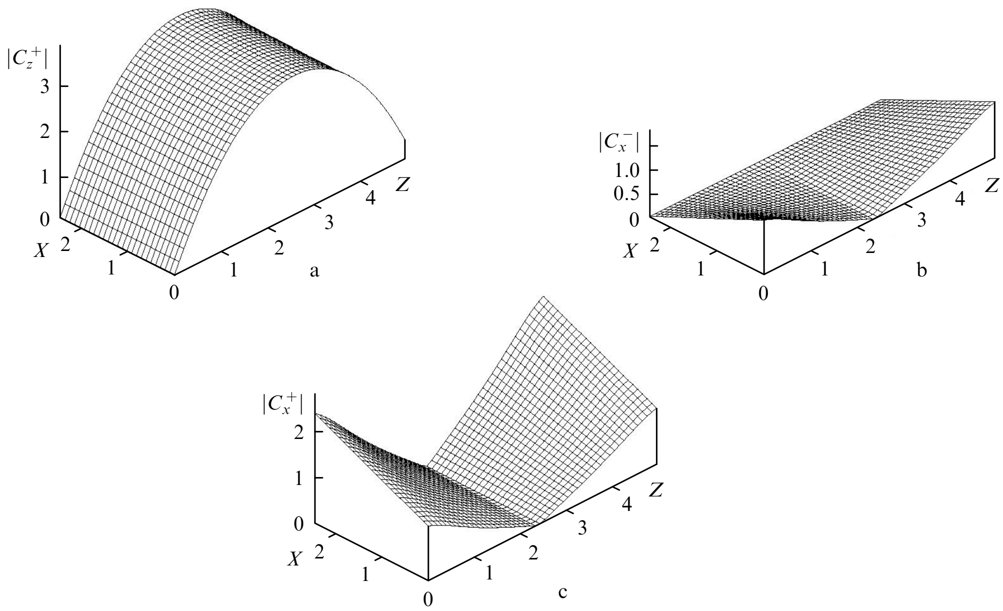

Figure 8. Spatial amplitude distributions of partial waves C_z^+ (a), C_x^- (b), and C_x^+ (c) in the stationary lasing regime in a system with an additional end mirror at $L_z = 5$, $L_x = 2.5$, $\beta\hat{T}_2 = 0.2$, $\hat{T}_1 = 1$. The main energy flux is carried out by the wave C_x^+ through the cross section $X = L_x$.

$R = 1$ in the stationary lasing regime. Under these conditions, up to 90 % of output energy is coupled out together with the wave $\hat{C}_x^+$ through the cross section $X = L_x$. Note that the mounting of an additional mirror does not deteriorate the phase-matching conditions, this installation being realised under the same geometrical dimensions of the laser as in the absence of the mentioned reflector.

4. Conclusions

We have shown in this paper that the two-dimensional DFB can be used to synchronise radiation of spatially developed laser medium in which amplification of a TE-polarised waves takes place. In the optical range, the new feedback mechanism can be realised based on the two-dimensional Bragg structure formed by a dielectric plate with a doubly periodic modulation of the thickness and providing coupling of TE- and TM-polarised waves propagating in mutually perpendicular directions. As a result of formation of additional wave flows of TM polarisation (and their distributed re-emission into the TE waves), radiation is synchronised in the direction perpendicular to the propagation direction of the amplified

References

1. Yariv A. *Quantum Electronics* (New York: Wiley, 1975).
2. Kogelnik H., Shank C.V. *J. Appl. Phys.*, **43**, 2327 (1972).
3. Kogelnik H., in *Integrated Optics* (Berlin – Heidelberg: Springer, 1979) Vol. 7.
4. Ghafouri-Shiraz H. *Distributed Feedback Laser Diodes and Optical Tunable Filters* (New York: Wiley, 2003).
5. Luk'yanov V.N., Semenov A.T., Shelkov N.V., Yakubovich S.D. *Kvantovaya Elektron.*, **2**, 2373 (1975) [*Sov. J. Quantum Electron.*, **5**, 1293 (1975)].
6. Morthier G., Baets R. *J. Lightwave Technol*, **9**, 1305 (1991).
7. Afanas'ev A.A., Mikhnevich S.Yu. *Kvantovaya Elektron.*, **34**, 315 (2004) [*Quantum Electron.*, **34**, 315 (2004)].
8. Baryshev V.R., Ginzburg N.S., Sergeev A.S. *Pis'ma Zh. Tekh. Fiz.*, **34** (3), 47 (2008).
9. Baryshev V.R., Ginzburg N.S., Malkin A.M., Sergeev A.S. *Opt. Commun.*, **281**, 4879 (2008).
10. Baryshev V.R., Ginzburg N.S., Zaslavskii V.Yu., Malkin A.M., Sergeev A.S., Thumm M. *Kvantovaya Elektron.*, **39**, 463 (2009) [*Quantum Electron.*, **39**, 463 (2009)].
11. Aversa C., Iizuka K. *IEEE J. Quantum Electron.*, **28** (9), 1864 (1992).
12. Andreev A.V. *Usp. Fiz. Nauk*, **33** (12), 997 (1990).